

X-711-74-193

PREPRINT

NASA TM X-70693

THE ATMOSPHERE EXPLORER POWER SUBSYSTEM

A. OBENSCHAIN
J. BACHER
P. CALLEN

(NASA-TM-X-70693) THE ATMOSPHERE EXPLORER
POWER SUBSYSTEM (NASA) 31 p HC [REDACTED] CSCL 22B

N74-28350

G3/31

Unclas
43336

JUNE 1974

Reproduced by
NATIONAL TECHNICAL
INFORMATION SERVICE
US Department of Commerce
Springfield, VA. 22151

GSFC

GODDARD SPACE FLIGHT CENTER
GREENBELT, MARYLAND

PRICES SUBJECT TO CHANGE

31P

**For information concerning availability
of this document contact:**

**Technical Information Division, Code 250
Goddard Space Flight Center
Greenbelt, Maryland 20771**

(Telephone 301-982-4488)

THE ATMOSPHERE EXPLORER POWER SUBSYSTEM

**A. Obenschain
NASA Goddard Space Flight Center
Greenbelt, Maryland**

and

**J. Bacher
P. Callen
RCA Astro-Electronics Division
Princeton, New Jersey**

June 1974

**Goddard Space Flight Center
Greenbelt, Maryland**

THE ATMOSPHERE EXPLORER POWER SUBSYSTEM

A. Obenschain
NASA Goddard Space Flight Center
Greenbelt, Maryland

and

J. Bacher
P. Callen
RCA Astro-Electronics Division
Princeton, New Jersey

ABSTRACT

The first in a series of three advanced design Atmosphere Explorer (AE) Spacecrafts was successfully launched into earth orbit on December 16, 1973. This paper will describe the design and operation of the power subsystem for the AE-C, D, and E spacecrafts. While the basic design of the power subsystem relies heavily on the flight proven ITOS and Nimbus designs, additional functional redundancy has been added in several component areas to improve the overall subsystem reliability. In particular, the battery charging technique has been modified to include third-electrode overcharge control; the automatic removal of all battery charge current is provided should abnormally high battery voltages (dependent upon battery temperature) be detected. An undervoltage detector has been added which removes all non-essential spacecraft loads should battery voltage fall below a given level. Also, the control circuitry of the shunt dissipator is redundant, and provides automatic removal of a failed shunt control amplifier; series redundant pass transistors are incorporated to prevent a single point failure from loading the solar array. All automatic functions can be overridden via ground command.

The geometric structure of the AE-C spacecraft is a 16-sided polygon approximately 155 centimeters (cm) in outside diameter and 120 cm in height. The sides and one of the two end surfaces of the structure are covered with 2 ohm-cm silicon solar cells, with 60 mil coverslides. The power subsystem supplies both an unregulated voltage bus, which varies from -26 to -38 volts, and a regulated -24.5 V ($\pm 1\%$) bus to the spacecraft loads. A shunt limiter maintains the maximum solar array bus voltage at -38.75 volts by dissipating excess array

power in resistance wiring mounted on the inside of the solar array substrate. Battery charge is supplied to each battery through an individual charger controller; during eclipse periods, and at those times when the load power demand exceeds the array's capability, load power is supplied from the batteries through series redundant discharge diodes.

Discussion pertaining to comparison between pre-launch predictions and actual flight performance of the power subsystem is presented.

CONTENTS

	<u>Page</u>
ABSTRACT	iii
MISSION DESCRIPTION	1
REQUIREMENTS	3
SUBSYSTEM CONFIGURATION	6
DESCRIPTION OF SUBSYSTEM COMPONENTS	6
Solar Array	6
Batteries	11
Power Supply Electronics (PSE)	12
Unregulated Bus Voltage Distribution	12
-24.5 Volt Regulated Bus	16
Battery Charge Control	16
Solar Array Shunt Regulator Control	18
Regulated Bus Detector	20
Unregulated Bus Undervoltage Detector	20
Baseplate Automatic Temperature Controller (ATC)	21
Fuses	21
IN ORBIT PERFORMANCE	
Bus Voltage/Protection Circuitry Performance	21
Battery Performance	22
Shunt Limiter Performance	22
Solar Array Performance	23
CONCLUSIONS	24
ACKNOWLEDGMENTS	25
REFERENCES	25

ILLUSTRATIONS

<u>Figure</u>		<u>Page</u>
1	AE-C Spacecraft	2
2	AE Spacecraft Configuration	4
3	Power Subsystem Basic Block Diagram	7
4	AE-C Spacecraft, Launch Configuration	8
5	Solar Array Output vs. Spacecraft Rotation Angle	9
6	Solar Array Current Sun vs. Angle	10
7	AE Signal Electrode Control Curves	13
8	Battery Charging Voltage Limit Versus Temperature	14
9	Power Supply Electronics Block Diagram	15
10	Block Diagram – Shunt Regulator	19
11	Solar Array Current Verses Time in Orbit	24

THE ATMOSPHERE EXPLORER POWER SUBSYSTEM

MISSION DESCRIPTION

The current Atmosphere Explorer (AE) program, which is a continuation of NASA's aeronomy research effort of the earth's atmosphere, consists of three spacecraft which will be launched over a 2-year period. The objective of the program is to investigate the photochemical process and energy transfer mechanisms accompanying the absorption of solar ultraviolet radiation in the earth's atmosphere by making closely coordinated measurements of the reacting components from a spacecraft which contains an on-board propulsion system to permit changing the height of perigee and apogee. The measurements to be made include the following:

- Extreme ultraviolet solar radiation.
- Neutral particle composition and temperature.
- Ion composition and temperature.
- Electron concentration and temperature.
- Photoelectron energy spectrum.
- Certain airglow lines.

The measurements will primarily be obtained in a largely unexplored low-altitude region between 120 and 300 kilometers (km), in order to define and clarify the chemical, energy absorption, conversion, and transport processes which control the structure of the upper atmosphere. Also, properties of the region above 300 km will be investigated, since most of the structural parameters of the high-altitude region are controlled as a result of the vertical transport by processes occurring below 300 km. The correlation of the high and low altitude measurements are of particular interest.

The AE-C Satellite (Figure 1) was launched from the Western Test Range on December 16, 1973 by a two-stage thrust augmented Delta launch vehicle into a highly eccentric orbit (4300 km apogee by 157 km perigee) having an inclination of approximately 68 degrees. The AE-C mission will consist of two distinct phases, identified as Phase I and Phase II. During Phase I, the spacecraft will

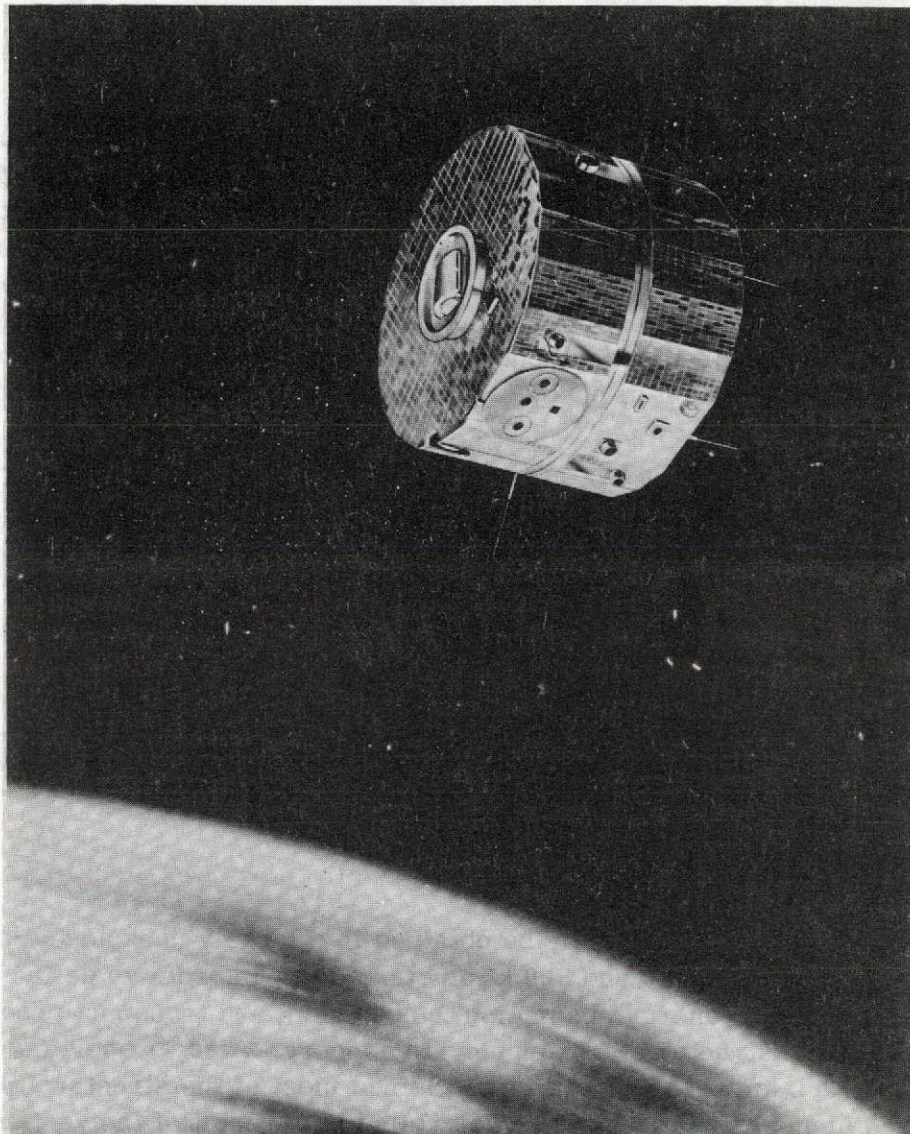


Figure 1. AE-C Spacecraft.

remain in the highly eccentric orbit. At intervals of about 2 to 4 weeks, special operations will occur, lasting for several days, in which the spacecraft perigee will be lowered in steps for brief periods through a range of 150 km to 120 km, consistent with spacecraft and instrument safety. This will be accomplished by firing the spacecraft propulsion system at or near apogee. At each perigee step, telemetry data will be acquired. During Phase II, the spacecraft will be placed into a series of circular orbits ranging between 250 km and 800 km. Phase I will last for approximately 8 months and Phase II will last for approximately 4 months.

The geometric structure of the AE-C spacecraft is a 16-sided polygon approximately 155 centimeters (cm) in outside diameter and 120 cm in height. The general configuration of the spacecraft is shown in Figure 2. The internal configuration consists of two baseplates separated by a central column and connected by six shear plates. Experiments and spacecraft equipment are mounted on one side of each baseplate. Six propellant tanks, belonging to the orbit adjust propulsion system (OAPS), are grouped symmetrically about the central column between the two baseplates. A momentum wheel assembly, used for spacecraft stabilization and spin control, is mounted on one end of the central column within the spacecraft with its attitude sensing mirror assembly protruding through a hole in the center of the upper surface. The experiments, mounted along the outer edge of the baseplates, are oriented to view the velocity vector, the zenith, or the general external environment. Sun pointing experiments are mounted within the +Z axis end of the central column. Accelerometers are mounted within the central column on the spacecraft spin axis. Solar cells mounted on the bottom and the sides of the outer shells will supply electrical power for the spacecraft and the experiments. Various sensors and probes extend through the outer skin to collect data and provide attitude control information.

A more complete description of the AE mission and spacecraft is found in Reference 1.

REQUIREMENTS

The AE power subsystem is designed to provide all electrical power to the spacecraft loads, with a design lifetime of one year. The basic power subsystem requirements are presented below; a more complete summary of the major subsystem performance requirements is presented in Table 1. (Unlike many spacecraft designs, the power requirements for AE are specified as watt-minutes (W-M) of experiment operating time per orbit: 4000 W-M at launch and 2000 after 8 months in orbit.)

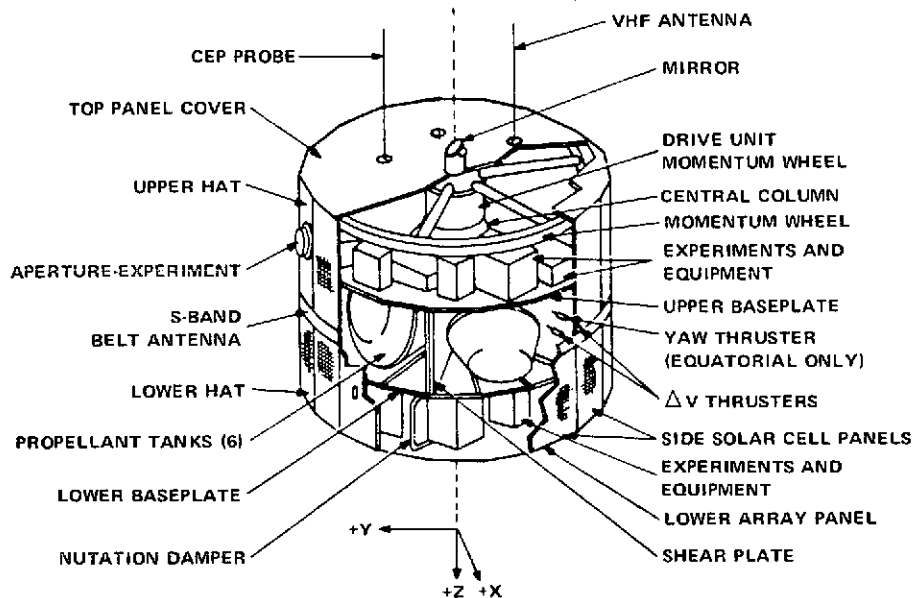


Figure 2. AE Spacecraft Configuration.

- Generate Required Voltage Busses - Negative Polarity
- Control Charging of Batteries
- Provide Shunt Regulation of Solar Array
- Provide Required Telemetry
- Provide Control of Spacecraft Heaters and Automatic Temperature Control (ATC) Subsystem.

While the techniques employed in meeting the basic power subsystem requirements are discussed in subsequent sections, it may be appropriate to review the requirement for a negative voltage distribution system. During the conception of the new AE spacecrafts, a basic groundrule followed was that a maximum amount of existing hardware design would be used. Many of the experiment and subsystem designs to be flown on the AE-C, D, and E spacecrafts were modifications of earlier AE and ITOS spacecraft designs which employed a negative voltage power bus. Likewise, the earlier AE and ITOS designs were, in large part, modified TIROS designs. (TIROS was a series of weather satellites developed by RCA and Goddard Space Flight Center during the late fifties and

Table 1
Power Subsystem Performance Requirements

Power Output: 4000 W-M of experiment operating time (BOL)
2000 W-M of experiment operating time (EOL)

Bus Voltage Distribution:

Unregulated load bus -26 to -38V
Regulated experiment bus -24.5V ($\pm 1\%$)
Pulse load bus - 26.0 to -35.5V

Maximum Voltage to Loads: -38.75V, worst case

Maximum Voltage Control:

- (1) Multiple power dissipating elements
- (2) Series redundant pass transistors in dissipating legs
- (3) Redundant Shunt limiter control circuitry
- (4) Automatic removal of a malfunctioning control circuit.

Load Control:

- (1) Redundant PWM Regulators
- (2) Automatic removal of non-essential spacecraft load when unregulated voltage falls below -25.7 volts
- (3) Automatic turn-off of regulated bus should voltage on bus exceed range -23.0 to -26.0 volts.

Battery Charge Control:

- (1) Individual charge controller for each battery
- (2) Current-limited battery charge at $C/4$ rate maximum
- (3) Voltage-Temperature taper charger characteristic
- (4) Third electrode cell overcharge control- reduce battery to $C/40$ when full recharge is accomplished (2 third electrode cells per battery)
- (5) Automatic termination of all battery charge should high battery voltages, dependent upon battery temperature, be detected.
- (6) Automatic termination of all battery charge if battery exceeds 37.5°C
- (7) Series redundant battery discharge diodes to preclude a single part failure from permitting uncontrolled battery charge.

Thermal Control: Active control of battery (spacecraft upper baseplate) temperatures to range of $10-13^{\circ}\text{C}$, nominal.

early sixties.) The TIROS series employed a negative bus system because, at the time of its development, it was difficult to obtain high gain NPN silicon transistors; PNP germanium transistors were used which required a negative bus system. As NPN silicon transistors became available, the existing design were modified to permit their usage, while still maintaining a negative bus system. Besides AE and ITOS, other GSFC satellites presently employing a negative bus distribution system include NIMBUS and ERTS.

SUBSYSTEM CONFIGURATION

A basic block diagram of the power subsystem is shown in Figure 3. The AE power subsystem provides all electrical power to the spacecraft loads. It consists of a solar array (mounted on two 16-sided substrates), three batteries and a power supply electronics (PSE) unit. The design is based heavily on previous Nimbus and ITOS power subsystems, although several improvements have been made over earlier designs. (For example, battery charger performance has been improved.) Power generated in the solar array is supplied to the spacecraft loads through an unregulated power bus, which varies between -26V and -38V. All loads which are normally powered during the complete spacecraft orbit, whether essential for spacecraft operation or not, are fed directly from the unregulated bus. Those loads which are normally only on during data collection phases of an orbit (e.g. tape recorder, experiments, etc.) are fed from a tightly regulated -24.5 volts bus. Battery charge power is supplied to each battery through an individual charge controller; during eclipse periods, and at those times when the load power exceeds the array's power generating capability, load power is supplied from the batteries through discharge diodes. The shunt limiter maintains the maximum unregulated bus voltage at -38V by dissipating excess array power in resistance wiring mounted on the inside of the solar array substrates.

DESCRIPTION OF SUBSYSTEM COMPONENTS

Solar Array

The solar array for the AE satellite is located on the sixteen side panels and one of the two ends—"bottom"—of the outer substrate of the satellite. The outer substrate is actually two removal be "solar hats", to which solar cell modules are bonded. Figure 4 shows the assembled spacecraft, with the two solar hats attached. The side array (both upper and lower portions) is composed of a total of 86 parallel strings, with 81 to 87 cells in series for a total

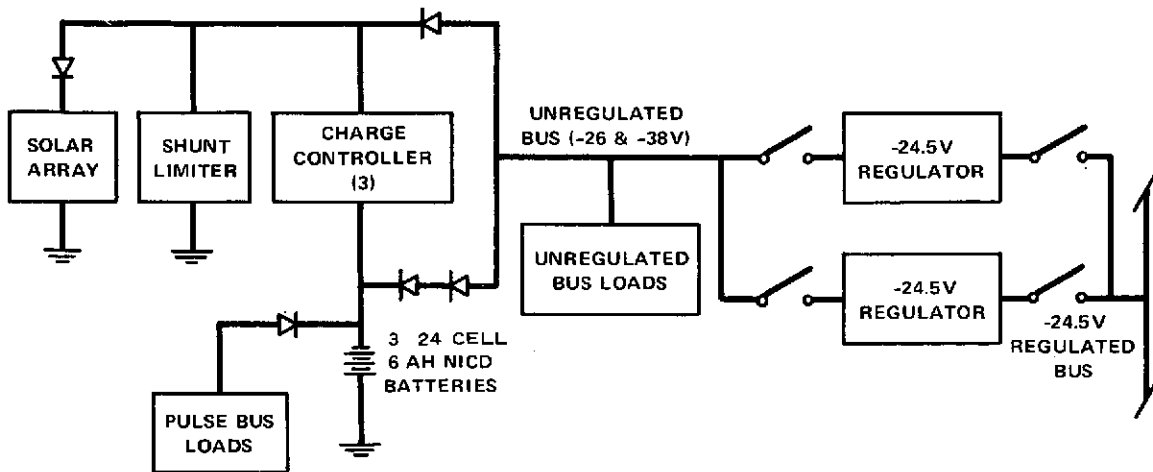


Figure 3. Power Subsystem Basic Block Diagram

of 7380 cells. The bottom solar array consists of 2508 solar cells: 20 parallel strings with either 125 or 126 cells in series. The output of the two solar arrays is paralleled inside the PSE.

The solar cells are nominal 2 cm \times 2 cm crucible-grown silicon cells, with a base resistivity of 1 to 3 ohm-cm. (The cells are slightly oversized, measuring 2.024 cm \times 2.024 cm, and are commonly referred to at GSFC as the "ERTS-cell".) The cells have an average base-cell efficiency of 11.7% at 0.46 volts and 28°C; minimum BOL maximum power is 61.2 mw. Each solar cell is covered with a .15 mm (60 mil) fused silica coverslide; the coverslides have an antireflection coating applied to the outer surface to enhance transmission of energy to the solar cell. A blue filter is applied to the lower surfaces of the platelet. The cut-in point (50% transmission) for the blue filter is 400 millimicrons \pm 15 millimicrons with less than one-percent average transmission characteristics from 300 to 370 millimicrons. Sylgard 182 silicon rubber adhesive is used to bond the coverslides to the solar cells. Interconnection between solar cells within a circuit is accomplished using an expanded silver mesh material 0.00508 mm (2 mil) thick. A fiberglass scrim cloth is used to isolate the solar cell circuits from the aluminum face-sheets of the solar hat substrates. The materials and fabrication techniques employed on AE have been used successfully for several years by RCA.

The required cut-outs in the solar hats - for experiment/thruster operations - and blank thermal surfaces result in a non-symmetrical array output characteristic, as shown in Figure 5 for three sun angles. (The "sun angle" of Figure 5 refers to the angle between the incident solar energy and the substrate normal.

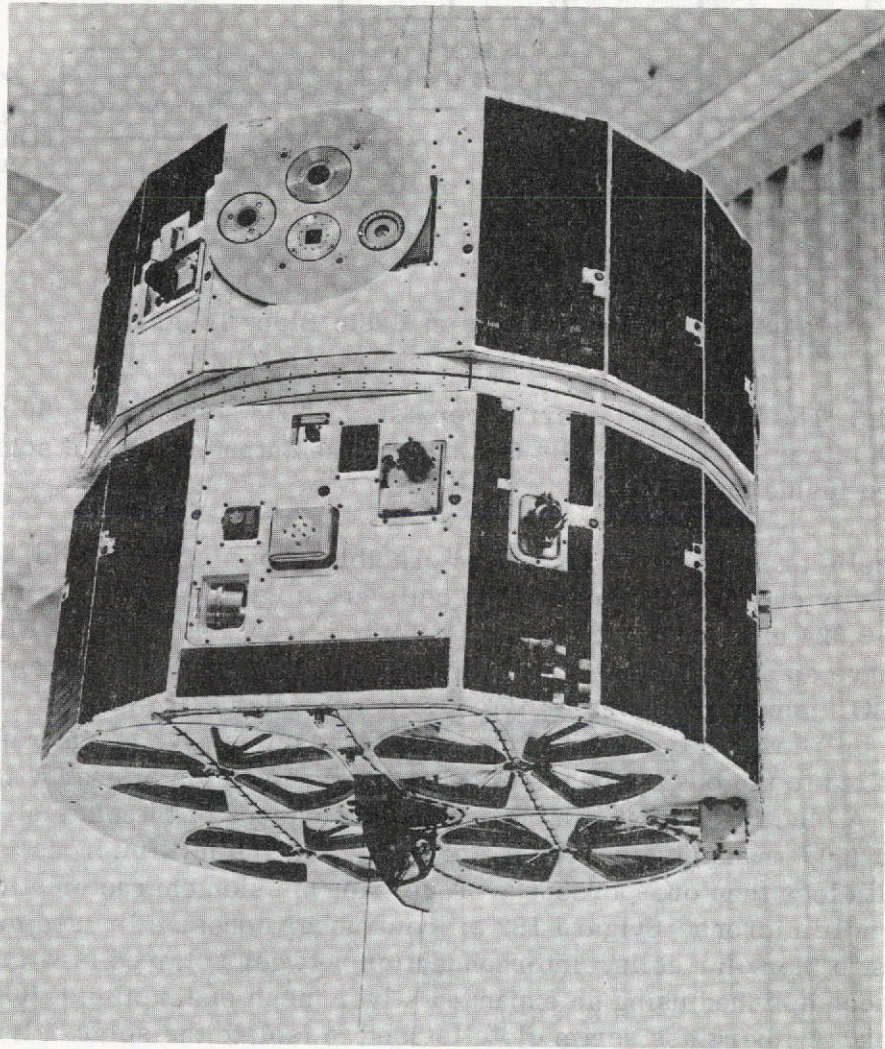


Figure 4. AE-C Spacecraft, Launch Configuration.

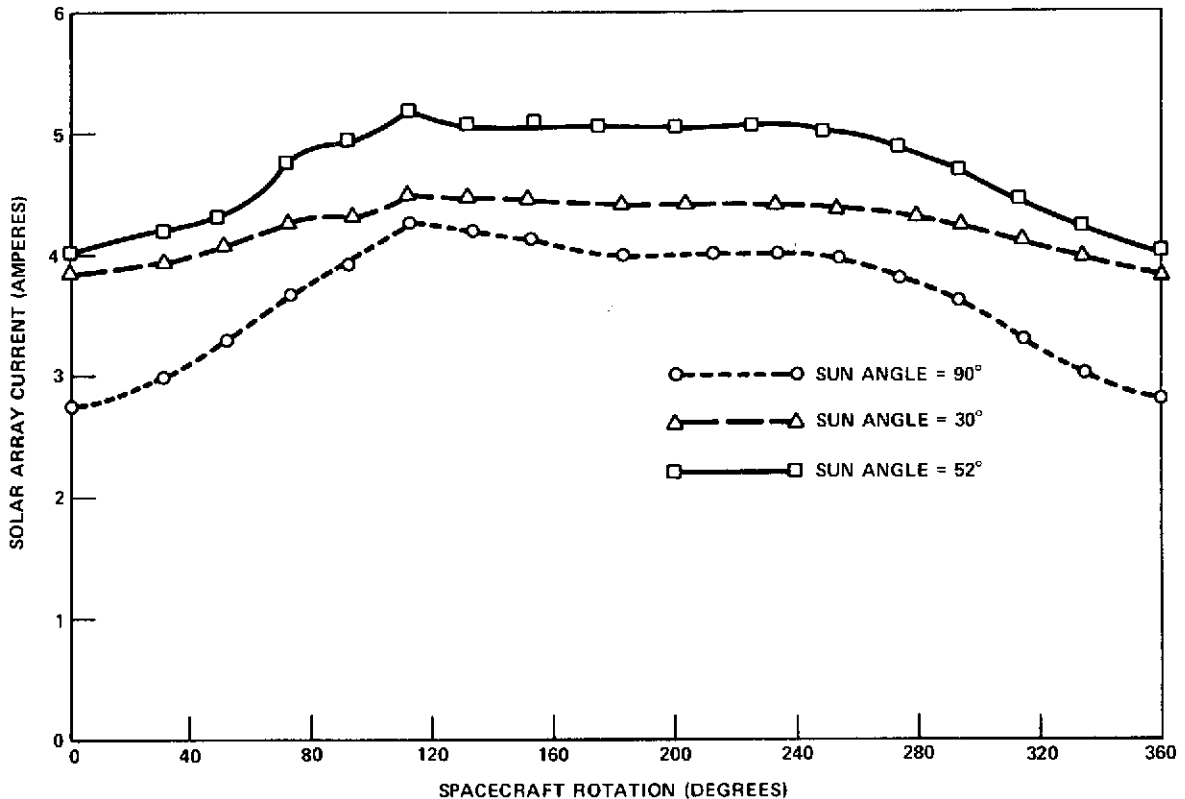


Figure 5. Solar Array Output vs. Spacecraft Rotation Angle.

Zero degrees means that the sun is looking directly at the bottom array of the solar hat, while 90° means that the sun is normal to the side of both the upper and lower array.) The output characteristic shown here is for the total array both side and bottom at BOL. The upper curve of Figure 6, BOL, gives the average current from the array output due to changes in sun angle. Charged particle irradiation damage causes a decrease in array output with life; the lower curve of Figure 6, EOL, shows the expected average solar array current output after 8 months in orbit. (Since the orbit will be changed from elliptical to low altitude, circular after 8 months no further radiation-induced damage is expected during the final four months of the mission.) While the decrease in current producing capability of the solar array is due primarily to radiation degradation, changes in the thermal characteristics of the array with life also account for a portion of the decrease.

The selection of the coverslide thickness used on AE was dictated both by the severe radiation environment experienced by AE - the spacecraft passes through the radiation belts twice each orbit during Phase I - and the spacecraft surface

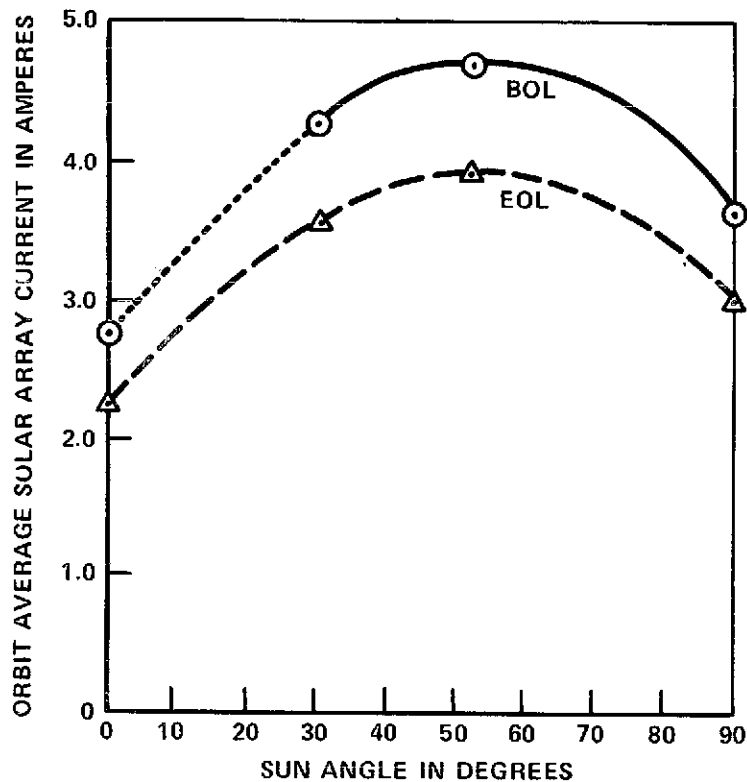


Figure 6. Solar Array Current Sun vs. Angle.

area available for placement of solar cells. An existing GSFC computer program² was used in the performance of a trade-off study which compared solar array output for various coverslide thicknesses with total array weight. It was found that use of the 0.15 mm coverslide resulted in a total integrated flux of 5.67×10^{14} 1 MeV electrons/cm² for 8 months in orbit. The associated decrease in array power (approximately 23%) still enables the power subsystem to meet the experiment duty cycle requirements at EOL.

While standard RCA fabrication techniques were employed in the construction of the AE solar array, the lack of GSFC experience with the thicker coverglassed cells led to a requirement that the exact AE design be qualified prior to fabrication of the solar array. The selected array design was qualified via a two-step test program. The initial phase consisted of a small test panel (1' x 2') being cycled three hundred times in air through the expected worst-case in orbit temperature extremes of -80°C to +120°C; no evidence of degradation was noted after this phase of the testing was conducted. The second phase was initiated in an attempt to simulate the effect of aerodynamic heating on the solar cell/coverslide assembly. The test panel was cycled 300 times from +20°C to 130°C

in vacuum, with a heat-up time of 30 seconds. The panels' cool down from 130°C back to 20°C took approximately 15 minutes. Post-exposure electrical testing and visual inspection again revealed no degradation in performance.

Batteries

The AE power subsystem contains these batteries; each battery consists of 24 series-connected nickel-cadmium cells, including two cells which contain signal electrodes. The cells have a rated capacity of 6 ampere-hours, and a nominal voltage of 1.25 volts. The battery contains thermistors for charge control, temperature telemetry, and for signal electrode temperature reference. The inter-cell series wiring is dual redundant. The 24 cells are packaged upright, in two parallel rows of twelve cells each.

The junction between each cell and the baseplate is insulated by a 0.005 inch layer of mylar film, with thermally conducting grease at the interfaces.

The top surfaces of the cells (including terminals) were coated with an organic coating, to prevent accidental short circuits, and to protect the cells from handling damage. The total battery weight is 8.9 Kg (19.6 pounds).

The battery cell is a nickel-cadmium rechargeable six-ampere hour aerospace cell, manufactured by General Electric. The separator is Pellon 2505 non-woven nylon, and the cell container is deep-drawn of 304L stainless steel. The average cell weight is 264 grams. The cell was designed to provide a minimum negative to positive ratio of 1.5:1, and this was verified on sample completed cells. The actual capacity is 7.0-7.5 ampere-hours, measured at the 3.0 ampere discharge rate to the 1.10 volt cutoff. Both electrodes are insulated from the cell container by ceramic feed-through terminals, manufactured by Ceramaseal.

Two cells in each pack contain a signal electrode, which is used to indicate when the battery reaches full charge. The signal electrode is in common electrolyte with the positive and negative plate stack. When connected to the negative terminal through an external resistor, a current flows in that circuit if oxygen is present. The oxygen pressure can thus be determined by reading the voltage drop across the load resistor. The magnitude of the signal electrode output is dependent upon the resistance of the load resistor, cell temperature, and oxygen pressure. The system is set so that when the temperature-dependent trip level is reached (due to oxygen evolution), the battery charge current will be reduced from full level or voltage-limited taper current to the trickle charge level. The system will remain under trickle charge (C/40) until the oxygen pressure decreases below the reset point.

The battery charge control system is based upon a primary current limit (C/4) with a temperature-sensitive voltage limit. The purpose of the signal electrode is to cause further reduction in charge current to the trickle level (0.150 amperes), in order to decrease the resultant over charge heating and gas evolution, and to increase battery reliability. Figure 7 shows the variation of signal electrode trip and reset point with temperature. The charge current will be reduced to the trickle level when either of the two signal electrodes in each battery reaches the trip point. The current will not be returned to the full charge (or voltage-tapered level) until the output of both electrodes is below the cutback point (also temperature dependent). Each battery is independently controlled.

In order to assure proper operation of the charge control system, the first group of cells received were subjected to test programs for characterization of charge voltage and signal electrode voltage. The charge voltage characterization test consisted of repetitive charge-discharge cycling to 18% depth of discharge (typical AE spacecraft operation). The V-T curve, lower curve of Figure 8, was selected to provide the desired C/D rated for a typical orbit.

The signal electrode cell load resistor value was selected after extensive characterization testing at the expected temperature extremes of the AE batteries. The relationship between pressure and voltage level was determined, for different load resistors. The greatest signal sensitivity was observed with a load resistor of 2000 ohms, particularly at the lower temperature range.

A more complete description of the battery charging system is provided in a later section of the paper.

Power Supply Electronics (PSE)

A block diagram of the PSE is shown in Figure 9. The major design changes in the AE PSE from its predecessors are in the area of subsystem protection; an attempt has been made to insure that spacecraft equipment failures do not degrade the power subsystem's performance.

The following presents a brief description of the operation of these functions.

Unregulated Bus Voltage Distribution

As shown in Figure 9 the unregulated bus is connected to both the solar array and the battery through blocking diodes; the connection with the solar array is through parallel redundant diodes, while each battery discharge leg contains two series redundant diodes. During the daylight portion of the orbit, the unregulated bus voltage telemetry reads 0.6 to 0.8 volts lower than the solar array

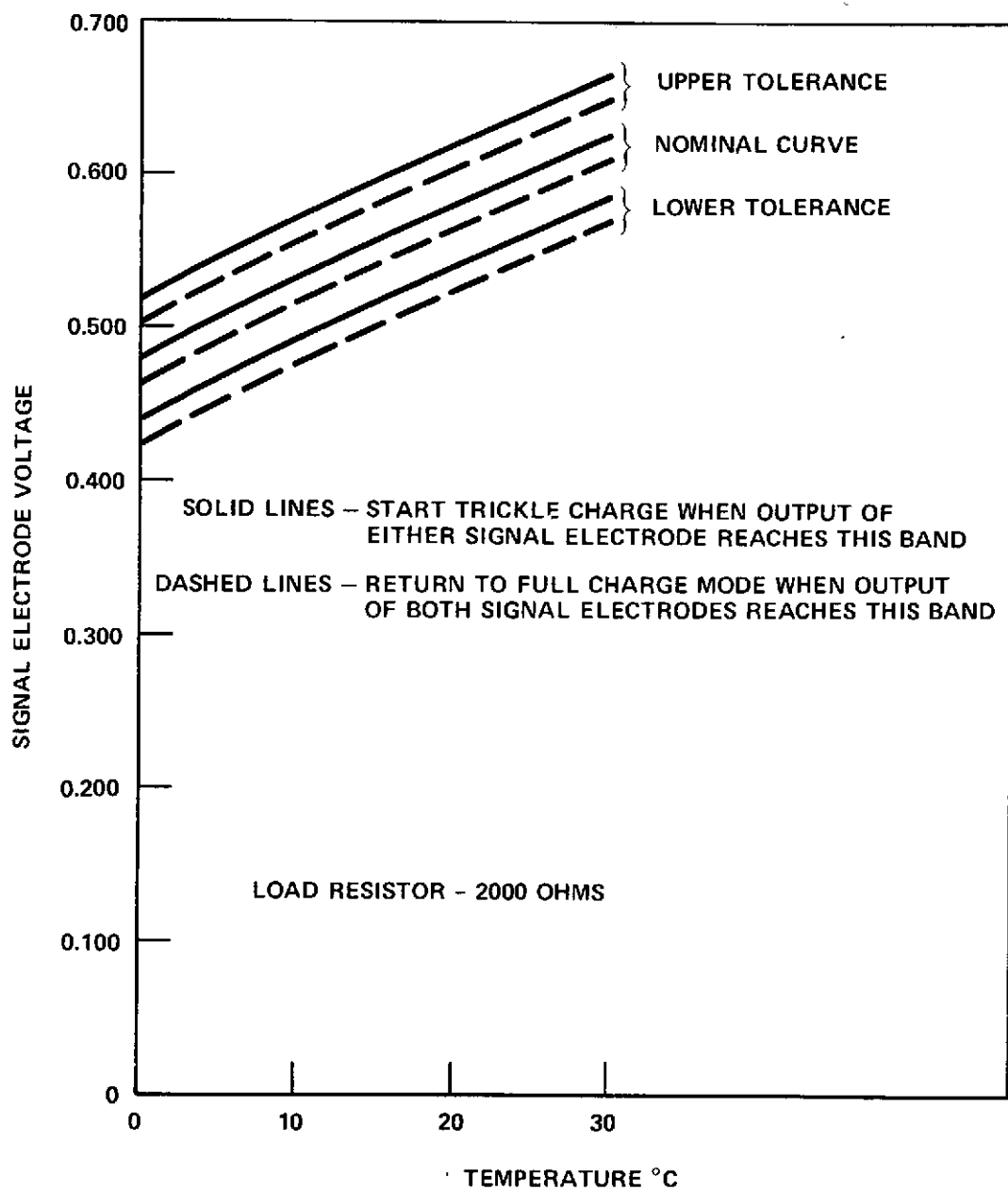


Figure 7. AE Signal Electrode Control Curves.

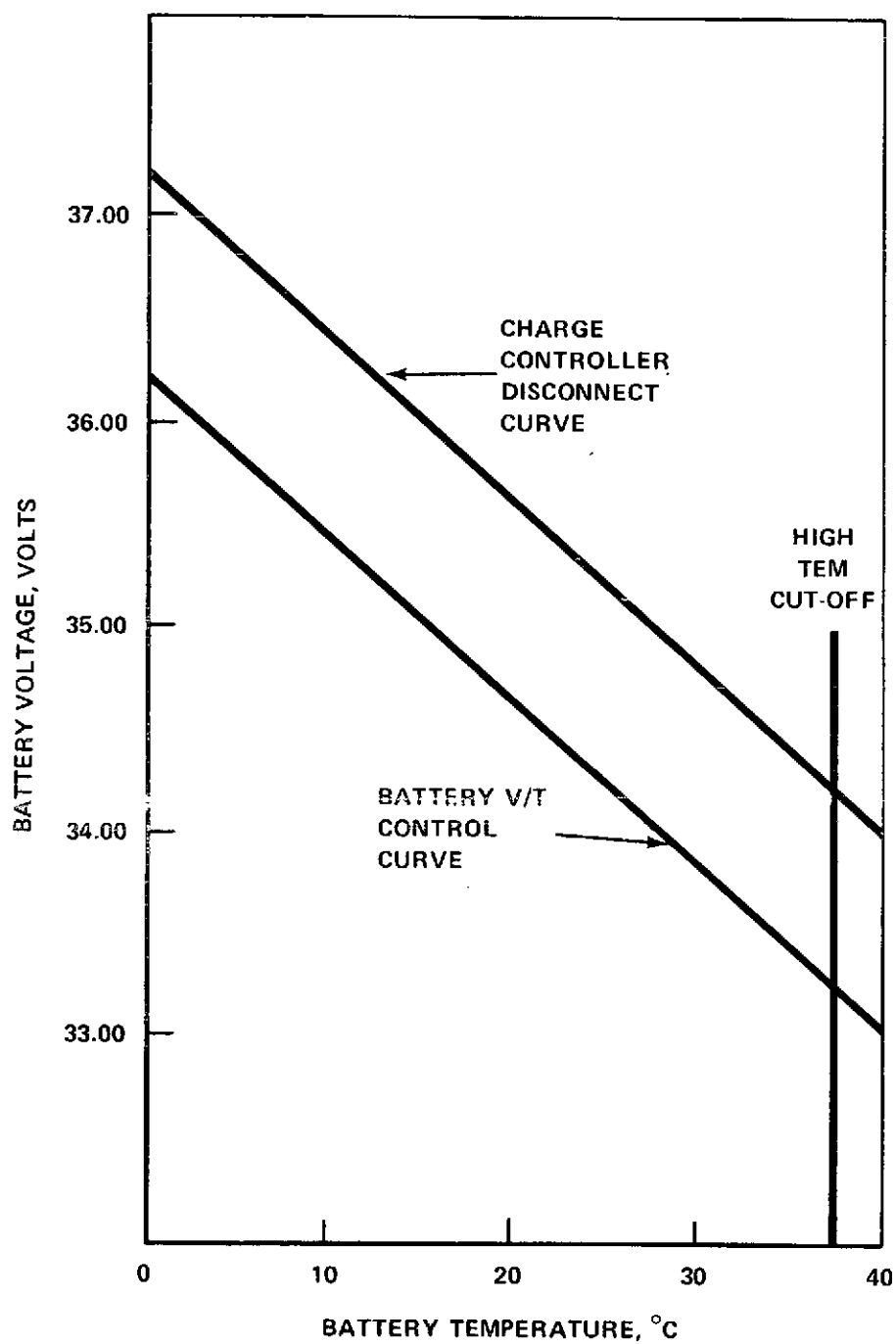


Figure 8. Battery Charging Voltage Limit Versus Temperature.

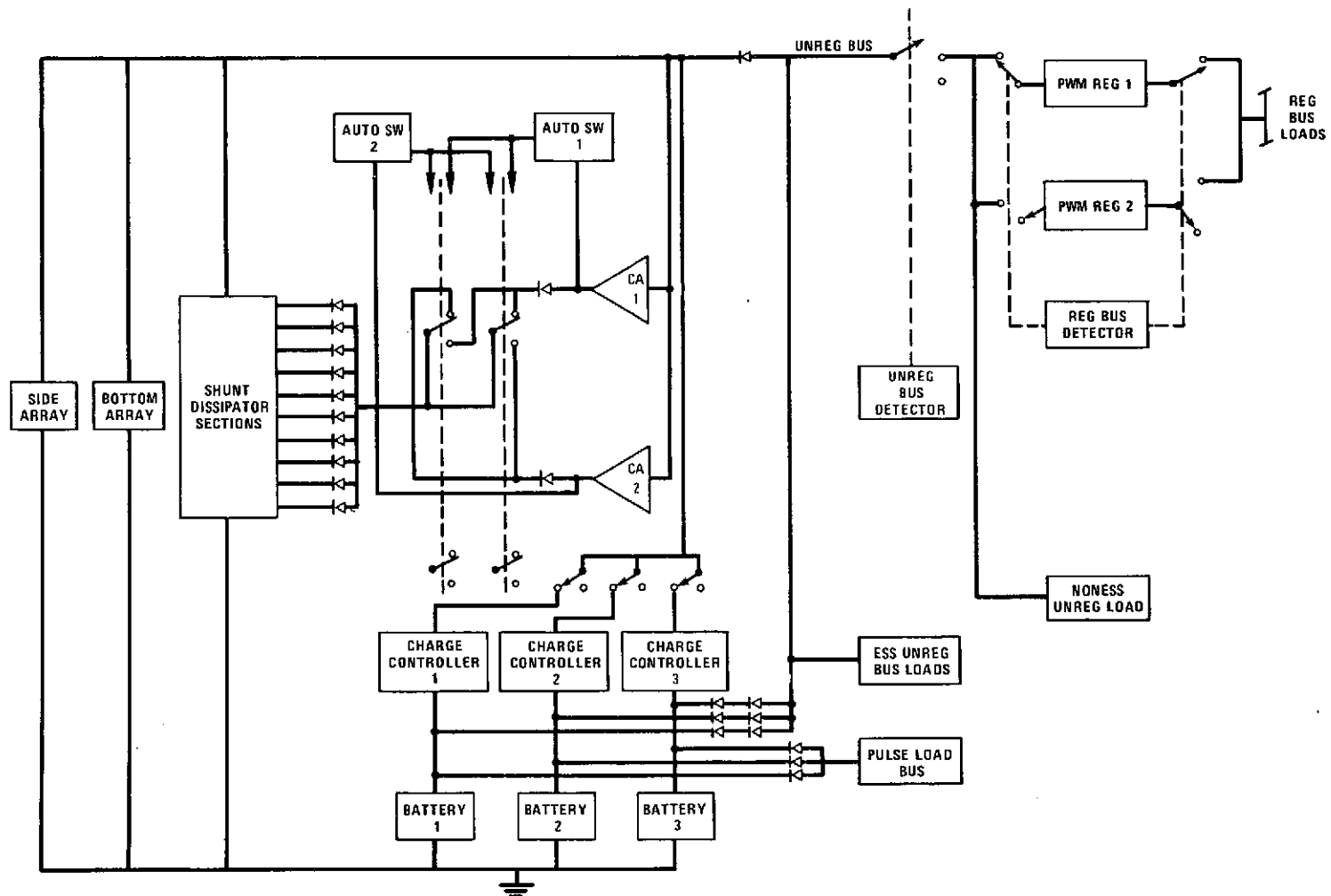


Figure 9. Power Supply Electronics Block Diagram.

bus voltage. At night, the unregulated bus is 1.0 to 1.2 volts lower than the battery voltage. Since the regulated bus, which contains the tape recorders and experiments, is usually not powered during the complete orbit, all loads which are required for normal spacecraft operation are powered from the unregulated bus through fuses. The addition of a series redundant diode in each battery discharge leg was made to insure that a single shorted diode does not permit uncontrolled battery charge.

The pulse load bus is formed by connecting the three batteries together within the PSE, and is used to power high current demand devices. Supplying power to devices such as squibs, thruster and tank valves, etc. from the unregulated or regulated busses would present unacceptable voltage spikes to the other spacecraft loads. The pulse bus loads are fused to protect the power subsystem.

-24.5 Volt Regulated Bus

The design of the pulse-width-modulated regulator for AE draws heavily on the proven Nimbus design. It permits the transfer of power from the unregulated bus to a regulated -24.5 volt bus with a 92% conversion efficiency at a nominal 6 ampere load. The unit is current-limited at 16 amperes, so that a regulated bus load failure can not damage the unit. Figure 9 shows that there are two identical regulators, only one of which can be connected at a time; of course, both regulators can be disconnected. To insure regulation within the required $\pm 1\%$ of -24.5 volts, it is necessary to have a minimum 400 ma load on the regulator when it is connected. This load is automatically connected whenever a ground command is sent to turn-on a regulator, and is commanded "off" when other loads (in excess of 400 ma) are applied to the regulated bus.

Battery Charge Control

The charge controller electronics charges each battery in an efficient manner and protects the battery from over-current, over temperature, over voltage (as a function of temperature), and excessive over-charge. Circuitry contained in the PSE provides these functions by monitoring and operating upon the following parameters:

- a. Battery charge current
- b. Battery voltage (as a function of temperature)
- c. Battery signal electrode voltage (third electrode oxygen-sensing device)

Normally, each battery will be charged at $C/4$ (1.5 amperes) when sufficient current is available from the solar array. When the voltage of the battery reaches a preset limit (temperature dependent), the charge current will be automatically reduced, to maintain the battery voltage at the desired limit. The current will decay to a value dependent upon voltage limit and temperature. The signal electrode's output will be used to reduce the steady state over charge current to a trickle value of $C/40$ (150 milliamperes).

The combination of voltage-temperature limit and signal electrode control is reliable because of long and successful experience with the former and extensive test data for the latter. This system combines the best features of each. The voltage-temperature limit does not drastically cut the charge current when the limit is reached, it merely reduces the current, according to the rate of voltage rise. The signal electrode control, which is used to reduce the current to $C/40$, will trigger after the cells have reached full charge and have started into the overcharge period.

The controller will operate in four normal modes, current regulator, voltage-temperature (battery voltage limit mode), battery signal electrode, and the hi-voltage, hi-temperature cutout mode. Each mode is discussed separately.

Current Regulator Mode—In this mode of operation, the charge controller operates as a current regulator, limiting the charging current to the maximum pre-established limit of $C/4$ (1.5 amperes $\pm 8\%$). This feature is unchanged from previous designs.

Battery Voltage Limit Mode (voltage-temperature)—In this mode of operation, the maximum voltage at which the battery can charge is limited. Also, the battery's maximum voltage limit is adjusted as a function of temperature, as indicated by the lower curve of Figure 8. The voltage taper curves have been lowered somewhat from the earlier ITOS and Nimbus designs.

Normally, at the beginning of charge, the state of the battery will require the controller to operate in the current limited mode. As the battery is charged, its terminal voltage is increased. Should the voltage-temperature combination exceed the limits, the controller senses this condition and acts to maintain the operating state of the battery within this mode. In this mode, the controller acts as a battery voltage regulator where the circuitry is designed to vary current in order to maintain control of battery voltage.

Battery Signal Electrode—Each battery contains two cells with signal electrodes which serve as a battery overcharge indicator. When the output from either of the third-electrode cells reaches the limit shown in Figure 7, the charge rate

is reduced to a nominal 150 ma level. This circuitry acts as a function of temperature; the higher the temperature, the greater the required signal electrode output.

When both cells indicate that the battery needs to be recharged, return to a normal (either current or voltage-limited) charge mode is made. This circuit can be disconnected via ground command should a failure occur which locks the charge into a trickle charge mode. Signal electrode cells had not previously flown on RCA/GSFC satellites.

Hi-Voltage, Hi-Temperature Disconnect Circuit—The charge controller will be disconnected from the solar array bus if the battery voltage, as a function of temperature, exceeds the voltage-temperature upper limit as shown in Figure 8. This is a new protection feature developed for AE.

When the battery voltage, as a function of temperature, or the battery temperature exceeds the limits in Figure 8 (upper curve), a Schmitt trigger is driven such that it actuates the disconnect relay, the relay is a latching type and a return to charge mode must be initiated by a ground command. Also included in the design is a high temperature cut-off circuit, which removes all battery charge current at a battery temperature of 37.5°C. In the event of circuit failure, the entire cutoff circuit may be disabled by another ground command.

Solar Array Shunt Regulator Control

The function of the shunt dissipator is to limit the solar array bus voltage to -38.75 volts by shunting excess solar array current. A block diagram of the shunt regulator is shown in Figure 10. Control of the maximum solar-array bus voltage is achieved by shunting current through the shunt dissipator sections when the control amplifier(s) sense an increase in solar array voltage above the cut-in level.

The shunt limiter consists of nine shunt dissipator power sections on the solar-array panels and two control amplifiers in the power supply electronics (PSE) unit. Only eight of the nine power sections are required to control the solar-array bus.

Sensing of the solar-array bus voltage is done by control amplifiers. Each control amplifier compares the solar bus voltage to a voltage reference and provides an output current which is proportional to the difference (error signal). The control-amplifier output current is fed through isolation diodes to a common bus and then through isolation networks to each of the power shunt dissipators,

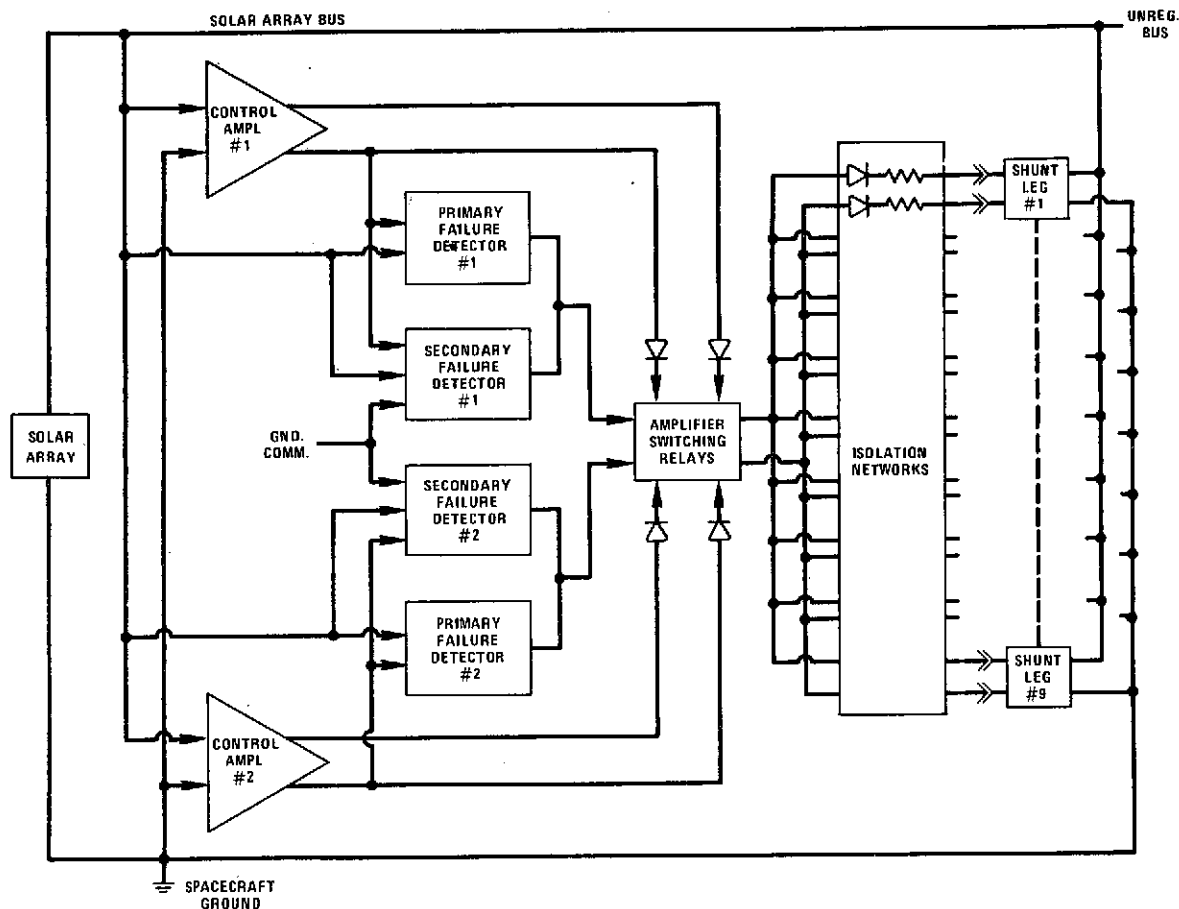


Figure 10. Block Diagram - Shunt Regulator.

which are located on the solar array. The shunt dissipator amplifies the control current causing some of the solar-array current to become shunt limiter current, which in turn decreases the solar bus voltage to a level where the control-amplifier error signal is minimized. The net effect is a closed-loop, negative-feedback control system which provides voltage limiting.

The control amplifier failure detection control protects the spacecraft against any failure in a control amplifier which would cause the shunt dissipators to be turned on in error. This is accomplished by detecting a simultaneous condition of solar array voltage less than 36 volts and the presence of control amplifier output current. Each of the two redundant control amplifiers is provided with an independent failure-detection control. A ground command is available to remove a "failed-on" control amp should the failure detection circuit fail to perform. The ground command is routed through a secondary failure detector which requires the simultaneous condition of solar array voltage less than -36 V

and the presence of control amp output current to allow the ground command to "gate" through. This is to prevent the inadvertant removal of a non-failed control amplifier in the event the redundant control amplifier has previously failed open; otherwise excessive solar array voltage could occur. An additional ground command is provided to permit the reconnection of a control amplifier that was automatically or ground-commanded "off".

Each of the nine dissipation legs is broken into two series sections, having a pass transistor associated with each. The use of serially redundant pass transistors precludes a single part failure from loading the solar array. The dissipation element is resistive wiring, bonded on the inside of each solar hat to distribute the generated heat evenly over the entire spacecraft surface.

Regulated Bus Detector

The regulated bus detector will automatically disconnect the on-line PWM voltage regulator if the regulated bus voltage leaves the range of -23.0 to -26.0 volts.

Voltage levels derived from the regulated bus are compared with a reference voltage by two differential amplifiers, one of which detects an overvoltage condition, and the other an undervoltage condition. The amplifier outputs are combined by an "OR" gate leading to a Schmitt trigger. If either amplifier detects an error, the Schmitt trigger changes state and actuates a relay in the regulated bus line, thereby disconnecting the on-line PWM voltage regulator. The regulator may also be switched on-line or off-line via the relay by ground commands. In the event of a circuit failure, the entire circuit may be disabled or enabled by two ground commands which drive a relay in the power supply line. The design of the circuitry relies heavily on proven ITOS and Nimbus designs.

Unregulated Bus Undervoltage Detector

The undervoltage detector will (a) automatically disconnect the on-line PWM regulator from the unregulated bus, and (b) provide a 40 msec pulse of unregulated bus power to the CDU, when the unregulated bus voltage falls below -25.7 V. The pulse to the CDU is used to remove all non-essential spacecraft unregulated bus loads.

A voltage derived from the unregulated bus is compared with a reference voltage by a differential amplifier. When the amplifier detects an error, the Schmitt trigger changes state and actuates a latching relay in the unregulated bus line. As a result, the relay disconnects the PWM regulator from the unregulated bus, and also supplies an AC pulse to a nonlatching relay, which supplies a momentary

relay closure to the CDU. The latching relay may also be switched to either state by ground commands. In the event of a circuit failure, the entire circuit may be disabled or enabled by two ground commands which drive a relay in the power supply line. The use of an undervoltage detector is unique to the AE design.

Baseplate Automatic Temperature Controller (ATC)

The baseplate ATC maintains the upper baseplate at a relatively constant temperature of either 12°C or 5°C - the desired baseplate temperature is selected via ground command - by opening/closing four louvers on the upper end of the spacecraft which permit the upper baseplate to "look" at space. The input to each of the four independent ATC circuits is a thermistor temperature input from the baseplate. If the baseplate thermistor temperature exceeds the selected temperature, a differential amplifier circuit in the PSE will sense an error and supply drive to an output amplifier, which in turn supplies power to open the ATC louver. If the ATC louver heater exceeds a preset temperature, all PSE drive to that ATC is removed automatically.

Fuses

The PSE supplies a 5 ampere fuse for each unregulated bus load, except the ATC's which have 0.25 ampere fuses. All regulated bus fusing is performed in the CDU. (Each of the power supply's bias regulators is also fused, but this power is only used internal to the PSE.)

An important feature of the PSE design is that all protection functions can be overridden via ground command. This insures that a failure in a protection circuit does not jeopardize the proper operation of the power subsystem.

IN ORBIT PERFORMANCE

Power subsystem performance during the first three months in orbit has been nominal, except for an anomaly in the shunt limiter protection circuitry which will be discussed in a later section. The following briefly describes the in-orbit performance of the AE power subsystem.

Bus Voltage/Protection Circuitry Performance

The solar array, unregulated and regulated busses have all been maintained well within specified limits. The maximum telemetered solar array bus voltage has been -38.5 volts, while the unregulated bus has varied between -37.8 and -27.0 volts. The regulated bus has varied from -24.8 volts, under light load conditions,

to -24.6 volts at maximum loadings. No bus protection circuits have actuated, except for the shunt limiter protection circuitry. No fuses, on either the regulated or unregulated bus, have blown.

Battery Performance

The three batteries have performed well. There is no evidence of cell divergence within a battery, and all these batteries "track" well during both charge and discharge. Battery voltages during charge and discharge all normal, averaging -34.5 volts and -31.0 volts, respectively. The battery temperature has been generally maintained in the desired 10° to 13°C range, except for periods of extended experiment duty cycles and worst-case thermal input: the minimum temperature experienced by the batteries has been 5°C, while the maximum was 21°C. The battery is subjected to a nominal 18% DOD, although periodic (approximately once per day) deep discharge (~50%) are experienced when extended experiment "on-times" occur.

Shunt Limiter Performance

While the performance of the shunt limiter has been nominal in that the maximum solar array voltages has been maintained within the required limits, periodic removal of one of the two redundant control amplifiers has occurred. Referring to Figure 10, it is seen that each of the redundant shunt limiter control amplifiers has an individual failure detection circuit associated with it. This circuit continuously monitors the solar array bus voltage and control amplifier output; if the output of the control amplifier exceeds acceptable limits, automatic removal of the "failed" control amp is provided. Analysis of the spacecraft operating condition when the disconnections occurred reveal that each event corresponded to an instantaneous peak load on the unregulated bus of magnitude greater than 500 ma.

A reassessment of the design of the failure detection circuitry reveals that the inherent response time of the circuit (~ 30 msec) is too fast; large pulse loads "fooled" the circuit into thinking that an out of tolerance condition was being detected. On future missions, the time delay of the protection circuit will be lengthened substantially to preclude an instantaneous change in bus voltage, associated with the large current change, from causing removal of the redundant control amplifier.

It should be stressed, however, that this anomaly in no way affects spacecraft performance as normal operation is maintained with only one control amplifier. Should an actual failure occur in the operating control amplifier, it is removed and the previously disconnected control amp reconnected; circuit design precludes

both amplifiers from being disconnected simultaneously. Operationally on AE-C, a command is routinely sent from spacecraft memory immediately after each large magnitude load change occurs which reconnects the control amplifiers. Since this operational procedure change has been implemented, no instances of control amplifier disconnection have been monitored on the ground.

Solar Array Performance

The performance of the AE-C solar array has apparently been as expected, although some uncertainty exists in the accuracy of the telemetered data. The difficulty in accurately analyzing the array's performance comes primarily from two sources: (1) inherent uncertainty in the accuracy of the telemetered data (2) limited viewing time of spacecraft housekeeping parameters each orbit. The first source of uncertainty was caused, in large measure, by the speed with which the AE-C spacecraft was integrated and tested; a final calibration of the solar array current telemetry was not possible prior to launch. The lack of final calibration, along with the inherent $\pm 3\%$ accuracy of the telemetry circuitry combined to yield a significant pre-launch uncertainty in the accuracy of the solar array current telemetry. After launch a computer program (Reference 3) was used to determine the true solar array current by comparing actual power subsystem performance with that predicted with various solar array outputs. The results of this analysis revealed that the telemetered array current contains a constant "off-set" of approximately 200 ma, with the actual value being higher than that monitored. Since this off-set does not appear to change with time in orbit, 200 ma has been added to each telemetered reading to arrive at the actual array value.

The second source of uncertainty arises because of the operational constraints imposed on the spacecraft by the experiments. To provide the maximum per-orbit experiment duty-cycle, complete orbit spacecraft housekeeping data is not collected; the only time available for looking at the operation of the power subsystem is during the real time station contacts. The difficulty with such an operational scheme is obvious: the operating condition of the power subsystem can only be analyzed when the spacecraft is in view of a ground station. On AE-C there are periods of time when the only contact with the spacecraft occurs during spacecraft eclipse, which of course makes array performance analysis impossible. During other periods of time the combination of solar array operating point, temperature and incidence angle essentially prevents any meaningful array performance analysis. Fortunately, there are periods in which array performance can be realistically determined at relatively constant operating voltages and temperatures, as shown in Figure 11. The solid line shows the pre-launch prediction, and the X's give the corrected values of the solar array current as monitored on the ground.

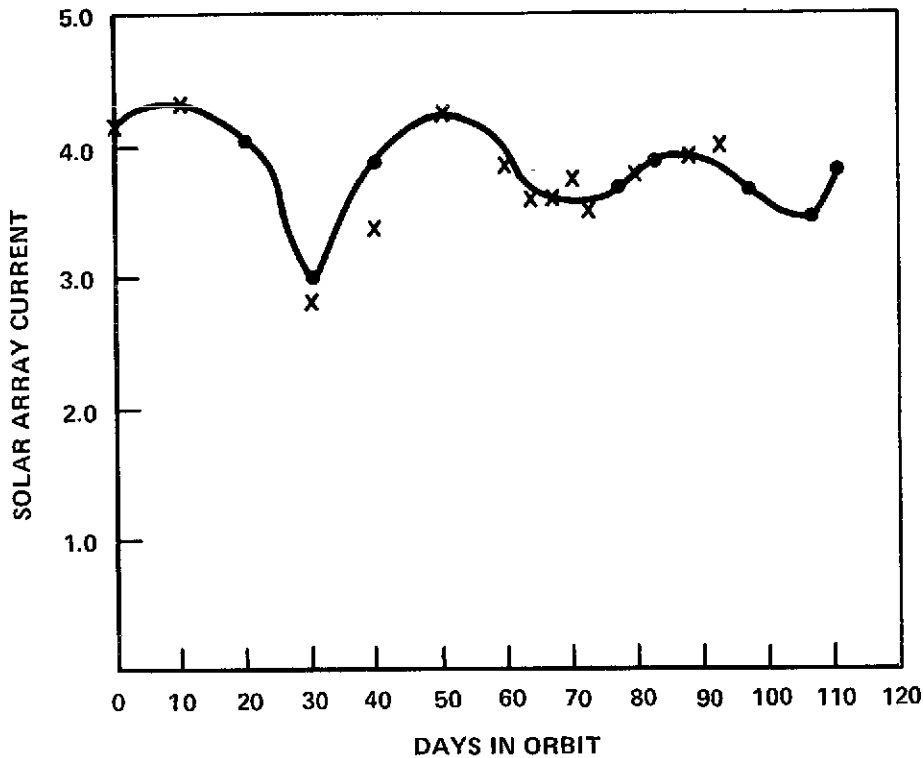


Figure 11. Solar Array Current Verses Time in Orbit.

Reasonable correlating exists between the measured values and pre-launch predictions except at 40 days in orbit. The exact cause of the rather large divergence between predicted and measured values is not understood. However, during the period which includes this datum point, thermal constraints on the spacecraft resulted in a reduced experiment duty cycle: there was no spacecraft eclipse, and the power subsystem was constantly in the shunt limiter operation (38+ volts on the array), with the array running at a higher than normal temperature. It is felt that the extrapolation of the solar array's operating condition from this high voltage/high temperature to the "normal" operating conditions used for comparison purposes may account for much of the apparent error. Solar array degradation during the first three months in orbit is approximately 18%, which is quite close to that predicted prior to launch.

CONCLUSIONS

Modifications have been made to the previous AE power subsystem design which greatly enhanced its reliability by adding functional redundancy in several key protection areas. Inflight performance confirms the beneficial aspects of the

design changes: a malfunctioning shunt control amplifier - an anomaly that could not have been corrected from the ground in previous designs - was reconnected via ground command, thereby eliminating any possibly deleterious effects of only one operational control amplifier. Solar array power degradation during the first three months in orbit was 18%, approximately the value predicted prior to launch. Bus voltage regulation and battery performance have been as expected.

ACKNOWLEDGMENTS

The authors wish to acknowledge the significant contribution of Elmer Holloway of RCA, who was responsible for the design of the solar array. Karen Posey, NASA/GSFC, developed the energy bookkeeping program which was used in the analysis of the in-orbit performance of the solar array. Edwin Moses of NASA/GSFC provided capable support in the evaluation of power subsystem in-orbit performance.

REFERENCES

1. D. W. Grimes, J. F. Coneybear, B. Stewart, "Some Design Aspects of the Low Perigee Atmosphere Explorers, C, D, and E," presented at the XXIV International Astronautical Congress, Baku, USSR, October 7-13, 1973.
2. A. F. Obenschain, "A Computer Program to Determine the Effects of Charged Particle Irradiation on Solar Cell Output Power", GSFC Document No. X-716-69-168, May 1969.
3. K. W. Posey, "The AE Energy Bookkeeping Program", Unpublished paper.